

SYNOPSIS ON
“INVESTIGATIONS OF XRF ATOMIC PARAMETERS AND ITS APPLICATIONS IN
ECOSYSTEM RESTORATION”



MAY – 2019

Submitted for the registration of

Doctor of Philosophy

DEPARTMENT OF APPLIED SCIENCES

CHITKARA UNIVERSITY

HIMACHAL PRADESH

Submitted by

VIJAY KUMAR GARG

(PHDASP17045)

Under the supervision of

Dr AJAY SHARMA

Faculty in Physics

Chitkara University

Himachal Pradesh-174103

INDEX

Sr. No.	Contents	Page No.
1	Introduction	3
2	Literature Review	3
	2.1 XRF Parameters	5
	2.1.1 Photo ionization Cross Section	5
	2.1.2 Fluoresce yield /Coster -Kronig yield	5
	2.1.3 Radiative Decay rates	6
	2.1.4 XRF Cross section	7
	2.1.5 Alignment Parameter	8
	2.2 XRF for ecosystem restoration	9
3	Justification For Research	12
	3.1 Motivation Of Research	12
	3.2 Research Gaps	13
4	Problem Statement	13
	4.1 Objectives	13
	4.2 Methodology	14
	4.2.1 XRF Technique	14
	4.2.2 Remediation of ecosystem	16
5	Expected Outcome	16
6	References	17

1. INTRODUCTION

Vacancies in inner shells of an atom are created when the atom is bombarded with photons / accelerated charged particles of appropriate energy. The creation of vacancy is known as excitation/ ionization and the atom becomes unstable. The vacancies decay within 10^{-12} s accompanying radiative and non-radiative emissions. The decay of vacancies is known as de-excitation. In radiative emission, vacancy created in inner-shell is filled by the jump of an electron from a higher/outer shell emitting photon known as X-ray of energy equal to the difference in binding energies of the involved inner and outer shells. In non-radiative emission, in the span of vacancy decay the difference in level energies disturbs an outer shell electron and knocks it out. This phenomenon is called Auger Electron emission and the emitted electron is called Auger Electron. Auger electron emission competes with X-ray emission. This process of photon induced vacancy creation and its decay with radiative emissions is known as X-ray Fluorescence (XRF), involves various parameters like photo ionization cross section, fluorescence yield/CK yield, decay rate, x-ray production/emission/ cross section and vacancy alignment etc. Energies of the emitted radiation, known as X-rays, from the atom are characteristic of the atom. Energy and intensity measurements of characteristic x-rays lead to elemental analysis as energy identifies the atom and intensity corresponds to numbers of the atom. Thus, investigations on the parameters are important for development / design of methods for elemental analysis based upon XRF technique .

Water, air and soil pollution results health risks that include diseases in almost all organ systems. About 40 percent of deaths worldwide are caused by pollution. In developing countries industrial sectors pose significant environmental and occupational health risks to populations (fig. 4). The pollutants of water are usually lead, mercury, fertilizer and pesticide compounds ,sewage and wastes from industries etc.



Figure 4 Environmental pollution in BBN area

X ray fluorescence spectrometry is a well established technique for elemental analysis at micro level. This is a non destructive technique and has sensitivity in ppm. It provides fast and simultaneous multi-elemental analysis for a sample [36]. The utilization of x-ray fluorescence technique for the determination of hazardous and essential trace element concentrations in environmental samples [soil, water and plants] is of immense importance.

2. Literature Review

In X-ray fluorescence, a photon of energy ($h\nu$) higher than the binding energy (B.E.) of an electron in a particular shell/sub-shell gets completely absorbed and an electron with kinetic energy equal to ($h\nu - B.E.$) is ejected out, the phenomena is known as photoelectric effect [1]. Photoelectric interactions occur with firmly bound electrons and their probability is the highest at the photon energy just above the B.E. of electron. Hence, the probability depends upon the energy of incident photon, atomic number of the element and the quantum state of the shell/sub-shell electron.

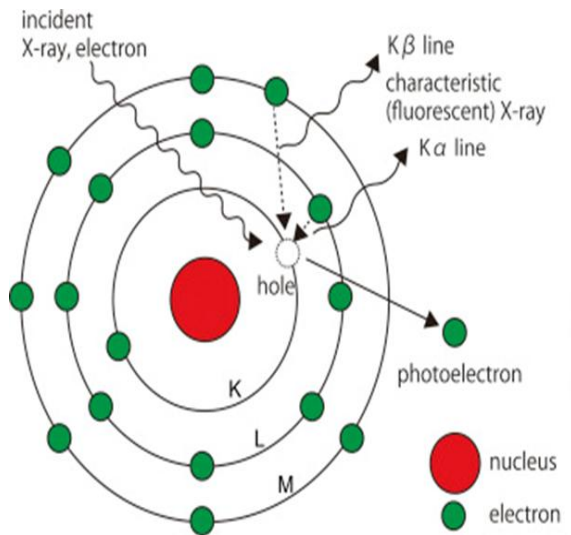


Figure 1 X-ray fluorescence illustration

As illustrated here a vacancy in K shell and its subsequent filling by radiative emission leads to characteristic K X-rays. Similarly filling of L/M or higher shell vacancies leads to L/M or higher shell X-rays. Further, the stronger lines in a given series are known as α lines and the weaker lines are called β , γ and so on as shown in Fig.2

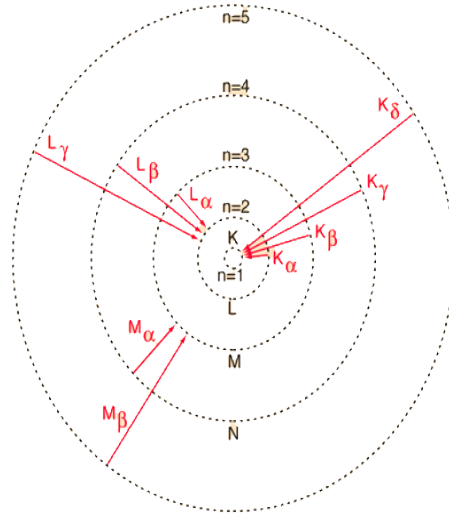


Figure 2 X-ray fluorescence emission lines

The normal transitions, known as diagram or normal X-ray lines, obey simple selection rules [2] viz.

$$\Delta n \geq 1$$

$$\Delta \ell = \pm 1$$

$$\Delta j = \pm 1 \text{ or } 0$$

where Δn , $\Delta \ell$ and Δj are the changes in the principal, orbital angular momentum and total angular momentum quantum numbers respectively of electron undergoing transition for the vacancy decay. The transitions, which do not obey the selection rules, are called non-diagram/forbidden/satellite lines.

2.1 XRF PARAMETERS

2.1.1 Photo-ionization Cross-Section (σ)

Photoionization cross-section (σ_i) determines the probability of ionization of an atom by photons in its shell/sub-shell. Different workers [3-6] have calculated the photo-ionization cross-sections using various theoretical models. Basic formula for finding K shell cross section is

$$\sigma_{K_i} = N_{K_i} / [I_0 G \epsilon_{K_i} \beta_{K_i} m].$$

where N_{K_i} is the measured intensity, I_0 is intensity of incident radiation, G is a geometrical factor, ϵ_{K_i} is the efficiency of the detector at the average K X-ray energy of the element, m is the mass per unit area of the element in g/cm^2 , and β_{K_i} is the self-absorption correction for the target material, which accounts for the absorption in the sample of the incident photons and the emitted characteristic X-rays.

Pratt et al. [3] produced K shell photoelectric cross-sections for the elements $13 < Z < 92$ in the energy range 200 keV-2 MeV. Storm and Israel [4] have made shell wise calculations in the energy range 1-100 keV. Among these Scofield [5] gave the theoretical total and shell/sub-shell photo-ionization cross-sections from 1-1500 keV for elements $1 \leq Z \leq 101$. On the experimental side, up to eighties, Pratt [6] has compiled most of the measurements. Karabulut et al.[7] measured K shell and L sub-shell photoelectric cross-sections in the atomic region $40 < Z < 68$ at 59.537 keV. Santra et al. [8] measured L sub-shell photo-ionisation cross-sections of Th and U at 22.6, 25.8, 29.2 and 32.9 keV. Software codes LSPICS and KCSPIF for generation of L subshell and K shell cross-sections have been produced by Sharma and Mittal [9] and Bansal and Mittal [10].

2.1.2 Fluorescence Yield (ω)/Auger yield (a)/Coster-Kronig Yield (f_{ij})

Fluorescence yield (ω) of an atomic shell/sub-shell is the fraction of the vacancies in the shell/sub-shell that is filled by X-ray emission i.e. the probability of filling of a vacancy through radiative transition in a shell/sub-shell. For K shell, fluorescence yield is the probability of K radiation and is given by

$$\omega_K = I_K / N_K$$

Where I_K is the number of emitted characteristic K X-rays and N_K is the numbers of primary K shell vacancies. Auger yield (a) is the probability that vacancy in the inner shell is filled through a non radiative emission of an electron from a higher shell. Coster_Kronig yield is the probability of shifting a vacancy from a subshell to higher subshell. In the presence of CK transition, fluorescence yield also get modified, and following relation hold good

$$\omega_i^X + a_i^X + f_{ij}^X = 1, \text{ where}$$

ω_i^X = Fluorescence yield for i th subshell of shell X, that is the probability that vacancy in i th subshell is filled through radiative transition.

a_i^X = Auger yield that is probability that vacancy in i th subshell is filled through a non radiative transition by an electron from a higher subshell.

f_{ij}^X = Coster-Kronig transition probability or yield is the probability that a vacancy in the subshell X_i is filled by electron making a transition from higher subshell X_j in the same shell X.

In L and higher shells with sub-shells, before filling of the created vacancy the vacancy may shift from lower to higher sub-shell of the shell. This non-radiative intra sub-shell vacancy transfer is known as Coster Kronig (CK) transition. Coster-Kronig yield f_{ij} is the probability of shifting a vacancy from a i th subshell to j th higher subshell.

In 1972, Bambynek and his co-workers [11] provided a comprehensive review on these yields. They compiled the experimental/theoretical status of the then present values. Krause [12] undertook a detailed

examination of available experimental and theoretical data on fine structure parameters ω_i , a_i and f_{ij} for L shell in the elemental range $12 < Z < 110$. Chen et al. [13] presented a comprehensive set for L sub-shell fluorescence yields for number of elements in the range $18 < Z < 100$ and Puri et al. [14] used logarithmic interpolation for the original Chen et al. [13] values and provided a complete set of fluorescence and Coster-Kronig yields for elements $25 < Z < 96$. For M shell, McGuire [15] calculated Coster-Kronig, Auger and fluorescence yields for elements from Ca-Th. Thomsen et al. [16] in 2007 measured fluorescence yields for elements $22 < Z < 42$ and observed an increase in the parameter with Z. Chen et al. [13] reported M4 and M5 sub-shell fluorescence yields and CK yields for elements $70 < Z < 100$ and CK transition probabilities and sub-shell fluorescence yields in M1, M2 and M3 sub-shells for the elements in the range $67 < Z < 95$ by Chen et al. [13]. Recently Kaur and Mittal provided codes for generation of theoretical data on M-subshell fluorescence and Coster Kronig yields and average M subshell yields.

2.1.3 Radiative Decay Rates (F)

Radiative decay rate (F) is the radiative fraction of total decay rate of the vacancies. The probability that $K\alpha$ radiation will be emitted rather than another K line is called Transition rate and is given by

$$F \text{ or } g_{K\alpha} = I_{K\alpha} / [I_{K\alpha} + I_{K\beta}] ,$$

where $I_{K\alpha}$, $I_{K\beta}$ are intensities of $K\alpha$ and $K\beta$ lines.

For K shell, it is easy to derive the but for L/M and higher shells, situation is difficult due to the involvement of number of sub-shells and the Coster-Kronig transitions among the sub-shells.

McGuire [15], calculated the L sub-shell radiative rates for the elements $11 < Z < 90$ and did similar calculations for M sub-shells in the elemental range $20 < Z < 90$. Crasemann et al. [17] calculated radiative transition rates for M shell vacancies for elements in the range $48 < Z < 92$. For M sub-shells, Bhalla [18] gave numerical values for radiative transition probabilities for elements $48 < Z < 93$ using relativistic Hartree-Fork- Slater model. Caliskan et al. [19] measured radiative vacancy distributions for the L2, L3 sub-shell and for M shell of some elements with atomic range $41 < Z < 68$. Bonetto et al. [20] measured L shell radiative transition rates for Gd, Dy, Er, Yb, Hf, Ta and Re by selective excitation of L shell with synchrotron radiation. Radiative vacancy transfer probabilities from Li ($i=1,2,3$) to M, N and higher shells for elements in range $77 < Z < 92$ has been measured by Sharma et al. [21].

2.1.4 X-Ray Fluorescence Cross-Section (σ^*)

X-ray fluorescence/ emission/ production cross-section (σ^*) is the probability of emission of X-ray after the decay of a vacancy created by the interaction of photon with atomic electron. It is a measurable

composite parameter defined as the product of photoionization cross-section (σ), fluorescence yield (ω), radiative decay rates (F).

$$\sigma^* = \sigma \omega F$$

Both theoretical and experimental data have been reported by different workers for K shell, L and M shell/sub-shell XRF cross-sections. Puri et al. [22] reported L XRF cross-section values calculated from the comprehensive set of physical parameters for elements $35 < Z < 92$. Mittal et al., [23] studied L X-ray Fluorescence cross sections for elements $40 < Z < 92$ at energies 2-116 keV. Ertugrul et al. [24] produced M X-ray production cross-sections from 1 to 1500 keV for elements with $70 < Z < 92$ and Chauhan et al. [25] did the same for elements with $67 < Z < 92$ at incident energies $E_{M1} < E_i < 150 \text{ keV}$ from different theoretical parametric data. A number of workers have measured L X-ray production cross-sections over a wide range of elements and energies. Sub-shell M X-ray production cross-section for M_{ξ} , $M_{\alpha\beta}$, M_{γ} and M_m groups for elements with $71 < Z < 92$ at 5.96 keV photon energy have been measured by Sharma et al. [26]. Bansal et al. [27] measured X-ray fluorescence cross-section for six elements in the range 78-92 at tuned synchrotron energies 5, 7 and 9 keV.

2.1.5 Alignment Parameter (A_2)

The state of an electron in the atom can be specified in terms of following listed quantum numbers along with their possible values.

Principal quantum number, n ; $n = 1, 2, 3, 4, \dots$

Orbital angular momentum quantum number, l ; $l = 0$ to $n-1$.

Spin angular momentum quantum number, s ; $s = \pm 1/2$

Total angular momentum quantum number, j ; $j = l + s$.

Total magnetic quantum number m_j : $m_j = -j$ to $+j$.

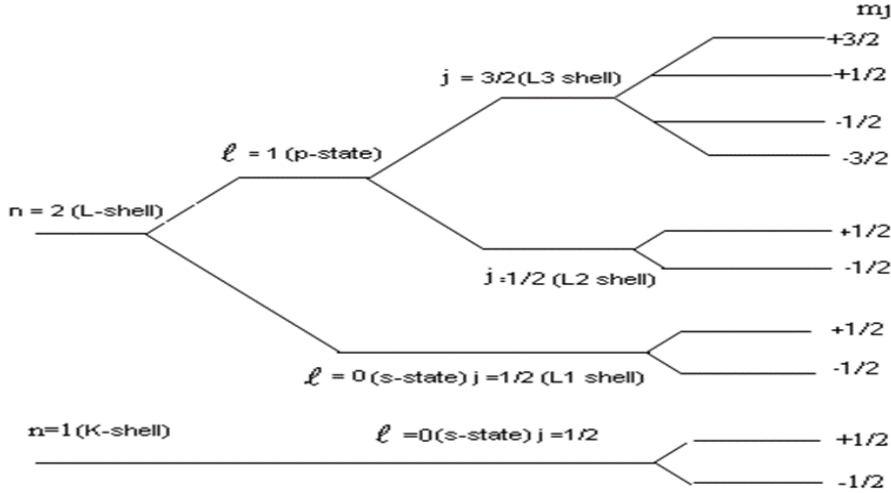


Figure 3 Electron distribution in magnetic states

The electron having total angular momentum quantum number j possesses $2j+1$ magnetic sub-states m_j varying from $-m_j$ to $+m_j$ as projections of j in the magnetic field direction (fig. 3). The parity and time reversal invariance imply that the ionization cross-sections for the $\pm m_j$ magnetic sub-states are same [28]. Thus, magnetic sub-states of each K, L1 and L2 state have equal vacancy distribution but some peculiar effect arises in L3 state as it has four magnetic sub-states $(-3/2, -1/2, +1/2, +3/2)$ and the vacancy population variance may arise in $m_j = 3/2$ and $m_j = 1/2$ states. This unequal population of vacancies in the magnetic sub-states of a state j is termed as alignment of atomic inner shell vacancy.

The fractional difference of ionization cross-sections for $m_j=3/2$ and $1/2$ magnetic sub-states of L3 state is represented by alignment parameter A_2 . [29]

$$A_2 = \frac{\sigma(L3, m_j = \pm 3/2) - \sigma(L3, m_j = \pm 1/2)}{\sigma(L3, m_j = \pm 3/2) + \sigma(L3, m_j = \pm 1/2)}$$

where $\sigma(L3, m_j=\pm 3/2, 1/2)$ are the photo-ionization cross-sections for the magnetic sub-states, $m_j=3/2$ and $1/2$. The alignment of atomic inner shell vacancy results in anisotropic emission of characteristic x rays.

The explanations regarding the influences of vacancy alignment in L3 state on subsequent decay processes led to two experimental methods for alignment determination, which are XRF based that is;

- a) Determination from production cross-section ratio for $L\alpha$ and $L\gamma$ groups of x-rays.
- b) Determination from angular distribution measurements.

Mehlhorn [30] in 1968 showed that characteristic x- radiation following the ionization of an inner electron by electron or proton impact should generally be polarized. Flugge et al.[28] were the first to predict the alignment of photon induced atomic inner shell vacancies and predicted significant anisotropy

in explicit calculations of the magnetic sub-state dependence of photoelectric cross-sections. In an excitation, the number of created vacancies may vary in different magnetic sub-states of a state with $j > 1/2$, which leads to vacancy alignment. In 1977 Berezhko et al.[31] did theoretical study of inner shell alignment of atoms in electron impact ionization and explained that it is spin-polarised. Auger electron spectroscopy of atoms can provide new information on both the Auger process and structure of atomic hole states. Sharma et al. [32] did experimental and theoretical anisotropy studies for tungsten and from the normalized angular L X-ray intensities (experimental and theoretical) for L_{β} and L_{α} peaks it has been observed that the experimental anisotropy is more as compared to the theoretical one. Recently, Sharma [33] studied inner shell alignment of atoms in photon impact ionization and observed that agreement of computed and experimental trends in the alignment parameter indicates that formulations used and interpretations given are valid. A critical comparison with the available results for Yb shows similarity in alignment trends. Gupta et al.[34] studied L3 vacancy alignment with single reflection set up using x-ray tube as excitation source. Measured alignment parameter shows variation with energy which notifies the existence of vacancy alignment in L3 sub-shell. In the latest measurements by Mehta et al [35], alignment of the vacancy states in case of L3 subshell in 82-Pb, 90-Th and 92-U elements, produced through the selective photoionization by the unpolarized 59.54 keV photons has been performed by using intensity measurements of the L3 subshell X-rays. The present precision measurements undoubtedly conclude that anisotropy in the L3 X-ray, if present, is very small and at the most of the order of theoretical calculated value.

So, all these parameters in their own ways/pattern influence the characteristic x-rays emission process and decide the intensity of emitted x-rays, that is the tool to quantify the element in a sample.

To check the existing prominent discrepancies in these parameters values in medium and high Z regions energy and intensity measurements will be undertaken with highly collimated intense synchrotron photons at RRCAT Indore, that leads to precision of measured data and certainty of results. The analytical use of data will be attempted for restoration of ecosystem.

2.2 XRF for Ecosystem Restoration:

As said earlier X-ray spectroscopy has immense applications in the field of trace elemental analysis of various samples. In case of environmental samples Richardson et.al.[37] in 1995 studied the XRF analysis of Lichen plants using this technique for elemental analysis. In 2002 Baranowsky et.al.[38] demonstrated the role of XRF in multielement soil analysis and Speciation analysis. Obtained result gave information on the main contents of soil anthropogenic activities which influence soil. In 2004 Bamford et.al. [39] using different kinds of XRF spectrometers had shown that elements ranging from Na to U can

be analyzed with little or no sample preparation using XRF and it is shown that analysis of environmental samples of soil, sediments, air aerosols, uranium contaminated soil and drinking water also exhibited the capability of XRF techniques for determination of trace and ultra trace elements. In 2006 Osan et.al.[40] studied multielemental Total reflection X Ray Fluorescence (TXRF) analysis of nanoparticles-effects of particle dimensions and load. In the hard X ray range (10.5 keV) the angular scans recorded on the Si wafers containing copper sulphate particles showed an angular dependence expected for particulate type deposition. Again Moreira et.al.[41] in 2006 showed that the technique SR-TXRF is so sensitive that certain elements which are not detected by other techniques can be detected using this technique including the elements Al, Cr, Ni, Cu, Zn, Ba and Pb. The technique was used to detect unexpected elements like Cr and Pb. Hence this work is pioneering project in the evaluation of ground water quality using Synchrotron Radiation-TXRF. In 2011 Misra N.L and Singh Mundher K.D [42] showed that because of attractive trace elemental analytical features, TXRF has a very promising potential for trace and major element determinations in nuclear materials. Small amount of sample avoid large radiation dose and generate less waste. The technique can be used to trace metal and non-metal elements in uranium oxide, thorium oxide and in mixed U-Th solutions. By using filters and secondary targets, the peak to background ratio can be increased in Energy Dispersive XRF (EDXRF). It results in better detection limit and requires small sample volumes. Sitko et.al.[43] in 2012 proposed empirical and theoretical methods, for quantitative XRF analysis depending on sample type, method of sample preparation, expected results and availability of standard samples. The fundamental parameter method is not as much accurate as only few standard parameters are available. Accuracy of both methods is same when same standards are used. In 2014 Margui et.al.[44] showed that with advances in instrumentation and preconcentration procedures, XRF spectrometry can offer new possibilities in the determination of trace elements in liquid samples. Recently in 2018 It has been shown by Tiwari [45] that XRR (X ray reflection) and GIXRF (Grazing angle incidence XRF) are powerful and complementary tools to characterize depth-resolved, surface– interface properties of nanostructured materials deposited on top of a flat smooth surface. The technique allows one directly to estimate average particle size, particle shape, nature of dispersion of nanoparticles on a substrate surface.

In 1995 Richardson et.al.[37], suggested XRF for trace-elemental analysis of Lichens plant. In the same year Melquiades et.al.,[46] used XRF technique for evaluation of heavy metal contamination in water and found it reliable for simultaneous multi-elemental analysis. Cheng et.al.,[47] in 2012 evaluated the reliability of portable XRF for heavy metal contamination soil samples and found that XRF technique is highly reliable in comparison to other method (i.e. AAS). Sunitha et.al.,[48] in 2012 studied the ground water contamination in agricultural land using XRF and found that ground water is much contaminated in

nitrate. Using same technique in 2013 Elzbieta et.al.[49] studied the effect of sewerage sludge on the accumulation of heavy metals in soil and their mobility to plants grown in it and showed that plants absorb Cd, Zn, Cu easier than Pb and Ni from the polluted land. In 2014 Margui et.al.,[44] measured the elemental analysis of liquid sample using TXRF and suggested this technique as more reliable for elemental analysis. Ali and Ateeg [50] in 2015 measured the soil pollutants near industrial sites in Sudan using XRF and found contamination of about 10 elements above pollution threshold limits. Ziwei et.al.[51] in 2018 measured the trace elements in agricultural land using AAS and their results indicate the accumulation of heavy metals in soil and fruit /vegetable.

3. Justification for Research

3.1 Motivation of Research:

A. Various atomic parameters affect the extent to which x-rays are produced by the target material to be studied. Very less data is available regarding study of transition probabilities, fluorescence yield, decay rates and fluorescence radiation absorption. Various factors affect these parameters to different extents. For example energy variation and angular distribution affects vacancy alignment studies of pure metals generally high Z elements like Pb, Th, U etc it can also affect XRF based elemental analysis of different samples to some extent. We know that vacancy alignment influences the subsequent decay processes and hence the related atomic parameters, therefore it is required to be determined accurately. If alignment is present then the related atomic parameters for example transition probabilities, fluorescence yield, decay rates and fluorescence radiation absorption may be affected when taken at different angles and energies. Therefore accurate determination of atomic parameters is very important as it may help in predicting exact nature of XRF spectra in case of elemental analysis. Also different groups determined atomic parameters and reported contradictory results in some cases [as is clear from literature], therefore it is very important to perform more detailed and precise synchrotron based XRF studies of atomic parameters in some high Z elements of experimental feasibility.

Furthermore, precise data on all these parameters for different elements is needed in the fields of atomic, molecular, radiation and nuclear, reactor physics, material science, dosimetric computation, elemental analysis of environmental, biological, geological samples, medical and engineering science and to check theory against experiment. Due to small difference in energy levels, fast Coster-Kronig transition probabilities and limited resolution of energy dispersive X-ray spectrometry (EDXRS), direct measurement of these parameters is not possible. Thus, experimental measurements on emitted X-ray intensities lead only to gross parameter, X-ray fluorescence/ production/ emission cross-section.

Therefore, to have comparison of theory with experiment, one has to calculate level to level parameters from experimental gross parameter. On the other hand, theoretical/semi-empirical data on fundamental parameters can be manipulated to have gross parameter value.

B. Solid hazardous waste and its dumping is a major issue in the entire state of Himachal Pradesh. Without exact information of quality and quantity of pollution sources present in soil and water, it is impossible to reduce or eliminate these pollutants. Hence for a holistic approach to environmental pollution studies, a wide range of representative samples need to be analyzed in sufficient quantities in order to exactly quantify and mitigate the toxicity present in agricultural areas.

Normal XRF/TXRF/AAS techniques for elemental analysis of environmental samples are being used with x-ray tube/radioactive sources.

Since Synchrotron radiation is a state of art technique with collimated intense radiation that gives speedy and accurate results in case of multi-elemental analysis, therefore, in the proposed work a step forward all experiments will be performed on highly advanced synchrotron radiation XRF/TXRF facility at BL-16 RRCAT-Indore. Chitkara University is already performing experiments in this direction at RRCAT.

3.2 Research gap

(A) Various Atomic parameters have been studied both theoretically and experimentally by various researchers, but only for particular range of elements and for certain amounts of incident photon energies. Data for heavy elements is less available and is needed to be studied, for example different groups performed alignment of inner shell vacancies studies and reported contradictory results, and therefore, our objective is to perform more detailed and precise study of XRF atomic parameters for some high Z elements using synchrotron radiations at selective excitations.

(B) Methodologies used for elemental analysis of environmental samples have their own merits/demerits in terms of precision and accuracy and it also depends upon choice of the sample. XRF/TXRF has proven itself as one of the most reliable methods for qualitative and quantitative analysis of environmental samples. Synchrotron based XRF/TXRF has many advantages over normal XRF. Our aim is to precisely identify the heavy toxic elements alongwith their concentration present in soil, water and plants located near the industrial units using synchrotron radiation based XRF/TXRF technique available at RRCAT and to propose remedial measures for stabilizing/elimination these toxins.

4. Problem Statement

4.1 Objectives

- To investigate XRF atomic parameters in some high Z elements more precisely using synchrotron radiations at BL-16.
- To precisely identify the heavy toxic metals along with their concentration present in soil, water and plants located near CETP site using XRF/TXRF technique.
- To explore the best management practices to mitigate soil and water contamination (after knowing the concentration of heavy metals present on the basis of XRF results). In this direction, the samples of soil, water and plants grown to be evaluated for heavy elements concentration and then after applying the different remediation methods the samples to be re-evaluated and compared with old XRF results in terms of toxicity.
- The research is also aimed at suggesting/recommending the most affordable and reliable method to stabilize/eliminate the pollutants.

4.2 Methodology

4.2.1 XRF Technique

Recently with the advancement of detectors and associated electronics, XRF has good detection limits and can determine almost all elements present even in small concentrations. Synchrotron radiation based XRF gives speedy, accurate and reliable results in case of multi-elemental analysis. No background and scattering effects appear specially in TXRF, therefore rapid and accurate observation with very small samples can be made possible.

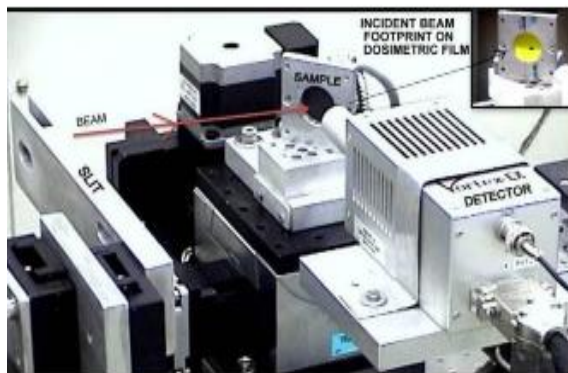


Figure 5. X-ray fluorescence set-up at BL-16 (RRCAT)

Since Synchrotron radiation is a state of art technique that gives speedy and accurate results in case of multi-elemental analysis, therefore, in the proposed work a step forward all experiments will be performed on highly advanced synchrotron radiation XRF/TXRF facility at BL-16 RRCAT-Indore. Chitkara University is already performing experiments in this direction at RRCAT.

In TXRF (figure 6) the direction of X-ray beam is almost parallel to the surface of the sample, so that X-ray beam is totally reflected. It avoid absorbing in the substrate, and significantly reduce the scattering, as well as the background noise.

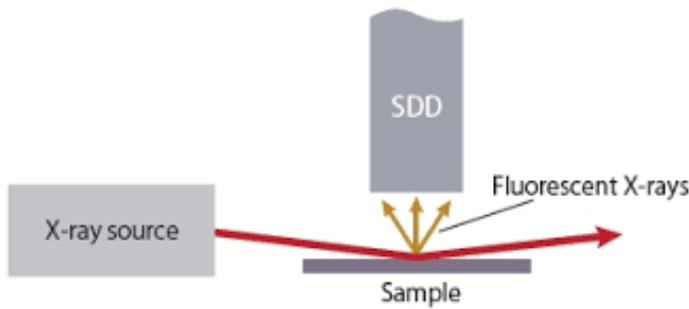


Figure 6. TXRF set-up

This method is preferred for liquid, powder samples and requires very small amount of sample even a drop/pinch of sample

XRF spectrum obtained in figure 7 (a) high pure W-74 sample and 7 (b) elemental analysis

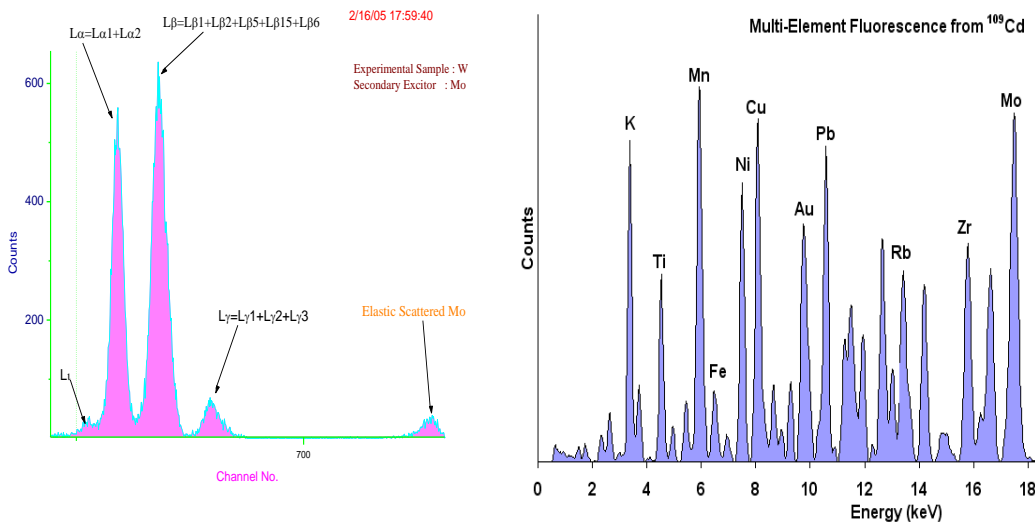


Figure 7 (a, b). X-ray fluorescence spectrum

4.2.2 Remediation of ecosystem:

Once the heavy metals are identified in contaminated soil, water, then the process of controlling/stabilizing the toxic elements will be proposed using the phytoremediation technique in which green plants are used to treat and control wastes in soil water and air

For remediation, nursery beds/agri. labs to be developed in the university campus for Soil to be procured from CETP site to nursery beds for phytoremediation.

Following are few reliable processes, which may be used in controlling the contamination.

Phytoionization	Phytoextraction	Phytofiltration
It is the process in which plants control spreading/movement of heavy metals in soil/water. The contaminated site is revegetated with plants e.g. grass and the pollutant can be stabilized [52].	It is the process in which plants can take up the heavy metals and concentrate them in their tissues. The plants can be harvested and disposed of safely. One type of plant used for phytoextraction is Indian Mustard [53] and is used to extract Lead from contaminated soil. Other plants that can be used for photoextraction include alfalfa, cabbage, tallfescue, juniper and poplar trees.	In this method heavy metal are removed directly from water by plant roots. The plants are grown directly in water or in water rich materials like sand using hydroponic method. In field experiments Sunflower plants have removed radioactive heavy elements directly from contaminated water.

All above methods are low cost and environmental friendly, therefore in the proposed work will be applied to mitigate pollutants from soil, water and hence plants grown.

5. Expected Outcome:

1. More precise values of atomic parameters related XRF and their contribution to elemental analysis will be known at various energies using synchrotron radiations at BL-16.
2. Information about the presence of heavy toxic elements and their relative concentration in the samples of soil, water and plants collected near CETP site will be known.
3. Remedial measures to stabilize/clean the heavy metals in soil and water will be explored.

6. REFERENCES:

1. Grieken V and Markowicz A, Handbook of X-Ray Spectrometry, 2nd Edition, (2002).
2. Jenkins R, An introduction to X-ray spectrometry, (1976).
3. Pratt R H, Levee R. D, Pexton R. L. and Aron W, Phys. Rev., 134 (1964) A898.
4. Storm E and Israel H I, Nucl. Data Tables, A7 (1970) 565.
5. Scofield J H, Lawrence Livermore Laboratory UCRL Report No. – 51362, (1973).
6. Pratt R H, Indian J. Phys., 58A (1984) 1.
7. Karabulut A, Gurol A, Budak G and Ertugrul M, Nucl. Instrum. Meth. B, 227 (2005) 485.
8. Santra S, Mitra D., Sarkar M., and Bhattacharya D, Radiat. Phys. Chem., 76 (2007) 1560.
9. Sharma A and Mittal R, 'Journal of Quantitative spectroscopy and radiative Transfer' 95, 1 (2005) 49
10. Bansal M and Mittal R, Radiat. Phys. Chem., 79 (2009) 583.
11. Bambynek W, Crasemann B, Fink R. W, Freund H U, Mark H, Swift C D, Price R.E and Rao P V, Rev. Mod. Phys. 44 (1972) 716.
12. Krause M O, J. Phys. Chem. Ref. Data, 8(1979)307.
13. Chen M H, Crasemann B and Mark H, Phys. Rev. A, 27(1983) 2989.
14. Puri S, Mehta D, Chand D, Singh N and Trehan P N, X-Ray Spectrom, 22(1993)358.
15. Mc Guire E J. Phys. Rev. A , 5(1972) 1043.
16. Thomsen V, Schatzlein D, and Mercurio D, Spectroscopy , 20 (2005) 22.
17. Crasemann B and Chen M. H. Phys. Rev. A 30, (1984)170.
18. Bhalla C P, J. Phys. B: At. Mol. , 3(1970) 916.
19. Caliskan B, Ertugrul M, Oz E and Erdogan H, J. Quant. Spectrosc. Radiat. Transfer , 74(2002) 139.
20. Bonetto R D, Carreras A C, Trincavelli J and Castellano G J, Phys. B: At. Mol. Opt., 37 (2004) 1477.
21. Sharma M, Kumar S, Singh P, Puri S and Singh N, J. Phys. Chem. Solids , 66(2005) 2220.
22. Puri S, Chand B, Mehta D, Garg M. L, Singh N and Trehan P N, At. Data Nucl. Data, 61(1995) 289.

23. Mittal R, Vandna S, Singh M, Journal of Quantitative Spectroscopy and Radiative Transfer, 68(2001)593.
24. Ertugrul M, Sade K and Erdogan H, X-Ray Spectrom, 33,(2004)136.
25. Chauhan Y, Kumar A and Puri S, At. Data Nucl. Data ,95(2009) 475.
26. Sharma M, Sharma V, Kumar S, Puri S and Singh N, Radiat. Phys. Chem.,75(2006)1503.
27. Bansal H, Tiwari M K, Mittal R, Journal of Quantitative Spectroscopy and Radiative Transfer, 204 (2018) 232.
28. Flugge S, Mehlhorn W, Schimdt V, Phys. Rev. Lett, 29(1972)7.
29. Oh S D and Pratt R H, Phys. Rev., 10(1974)1198.
30. Mehlhorn W, Phys. Lett. A, 26 (1968)166.
31. Berezhko E G, Kabachnic N M, J. Phys. B At. Mol. Opt. Phys., 10(1977)2467.
32. Sharma A, Mittal R, Nuc. Instr. Meth. Phys. Res. A, volume 619 (2010) 55.
33. Sharma A, Journal of electron spectroscopy and related phenomenon, 225 (2018) 1.
34. Gupta S, Deep K, Jain L, Ansari M A, Mittal V K and Mittal R., Appl. Radiat. Isotopes., 68(2010) 1922.
35. Mehta D, Gurjeet S, Gurjot S, Upmanyu A, Harpreet S K, Kumar S, Eur. Phys. J. D, 71(2017) 248.
36. Tiwari M K, Lodha G S, Sawhney K J S, Gowrisankar B, Singh A K, Bhalerao G M, Sinha A. K, Arijeet, Verma A, Nandedkar, R V, Current Science 95(2008) 603.
37. Richardson D H S, Shore M, Hartree M, Richardson R M, The Science of Total Environ., 17697(1995)105.
38. Baranowski R, Rybak A, Baranowska I, Polish Journal of Environmental Studies, 11 (2002) 472.
39. Bamford S A, Wegrzynek D, Chinea-Cano E, Markowicz A, Nuklionika, 49 (2004) 87.
40. Osan J, Török S, Beckhoff B, Ulm G, Atoms. Environ., 40 (2006) 4691.
41. Moreira S, Ficarís M, Elisa A, Vives S, Instrumentation Science and Technology, 34 (2006) 567.
42. Misra N L, Singh Mundher K. D, Progress In Crystal Growth and Characterization of Materials, 45 (2002) 65.
43. Sitko R, Zawisza B, Electrochimica Acta Part B, 62 (2012) 777.
44. Margui E, Zawisza B, Sitko R, Trends in analytical chemistry, 53 (2014) 73.
45. Tiwari M K, Spectroscopy Europe, 30 (2018) .
47. Melquiades F L, Appoloni C R, Journal of radioanalytical and Nuclear Chemistry, 262 (2004) 533.
48. Cheng M W, Hung T T, Kai H Y and Jet C W, Environmental Forensic, 13 (2012) 110.
49. Sunitha V, Muralidhara B R, Ramakrishna M R, Advances in Applied Science Research, 3 (2012) 1618.
50. Elżbieta W, Urszula W, Andrzej B, Tadeusz Ł, Environmental protection Engineering, 39(2013) 68.

51. Ali I H, Ateeg A A, Int. J. Environmental Reseach, 9 (2015) 291.
52. Ziwei D, Yang L, Qingye S, Haojie Z, Int. J. Envir. Res. And Public Health, 202 (2018) 1.
53. Zhitong Y, Jinhui L, Henghua X, Conghai Y,Procedia Environmental Sciences, 16 (2012) 722.
54. Lambert M , Leven B A, Green R M, Mol. Cell Biol.,17 (1997) 3966.